

In the format provided by the authors and unedited.

Centennial glacier retreat as categorical evidence of regional climate change

Gerard H. Roe

Dept. Earth and Space Sciences, University of Washington, Seattle, WA.
gerard@ess.washington.edu

Marcia B. Baker

Dept. Earth and Space Sciences, University of Washington, Seattle, WA.
mbbaker@ess.washington.edu.

Florian Herla

Institute of Atmospheric and Cryospheric Sciences, University of Innsbruck, Austria
Florian.Herla@student.uibk.ac.at.

1 Similar results from alternative glacier models

2 In this section we demonstrate that an alternative glacier model gives similar answers to the three-
3 stage model^{S1} used in the main analysis. The three-stage model provides enhanced performance
4 at high frequencies (i.e., $f > 1/(2\pi\tau)$) compared to an earlier class of analytic models that used
5 a simple relaxation model of glacier dynamics (a *one-stage* model), represented by a first-order
6 differential equation^{S2,S3}.

$$\left(\frac{d}{dt} + \frac{1}{\tau}\right)L' = \beta b'(t), \quad (\text{S1})$$

7 Eq. (S1), and closely related equivalents, have been widely used in studies exploring glacier response
8 to climate change^{S4,S5,S6}. As such it is worth showing that, within our framework, one could use
9 either Eq. (3) or Eq. (S1) and obtain similar results. For this one-stage model the equivalent
10 solutions to Eq. (5) and (7) are:

$$\phi_1(t_o, \tau) = \tau \cdot \left[1 - \frac{\tau}{t_o}(1 - e^{-t_o/\tau})\right], \quad (\text{S2})$$

11 and

$$\psi_1(\tau) = \tau \cdot \sqrt{\frac{\Delta t}{2\tau}}. \quad (\text{S3})$$

12 and so the equivalent amplification factor for the one-stage model is given by $\gamma_1(t_o, \tau) = \phi_1(t_o, \tau)/\psi_1(\tau)$.

13 Figure S1 compares the γ s from the one-stage and three-stage equations and demonstrates that,

14 for both models, $\gamma \sim 5$ to 6 in the parameter space applicable to alpine glaciers and century-scale

15 climate trends. The value of γ for the one-stage model is slightly higher than for the three-stage

16 model because, for a given τ , the one-stage equations respond more quickly to a trend. How-

17 ever, the essential point is that the detailed dynamics do not matter much - physical systems with

decadal response times will act as sensitive amplifiers of centennial-scale climate change. We note

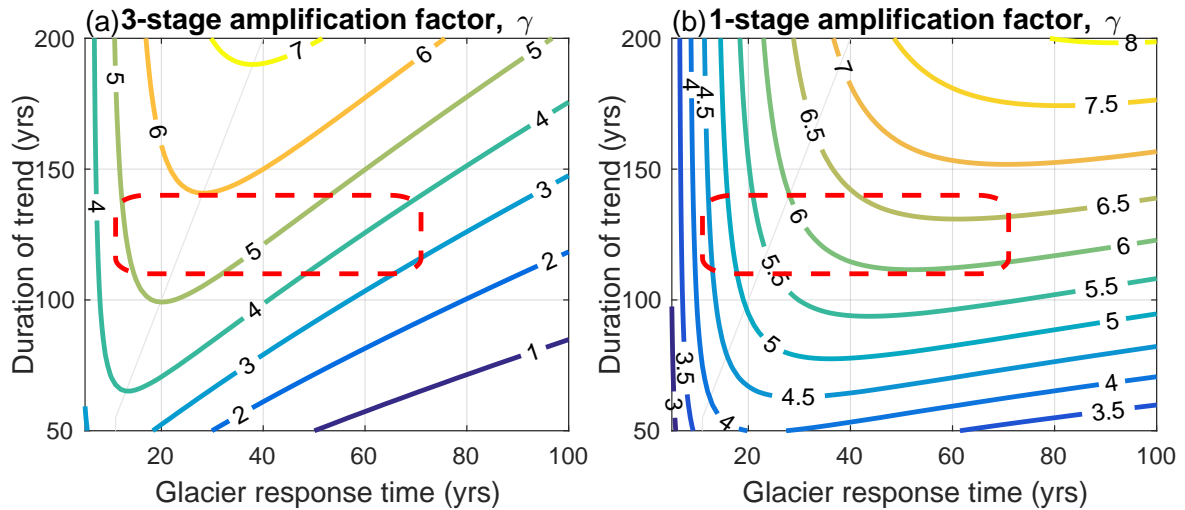


Figure S1: Amplification factor γ in the relationship $s_L = \gamma \cdot s_b$, contoured as a function of the glacier response time and the duration of the applied trend. (a) γ for the 3-stage model (Eq. 8), reproducing Figure 2b; (b) γ for the 1-stage model (Eq. S1). The red-dashed box shows the range of parameter space that applies for typical alpine glaciers and centennial-scale climate trends from anthropogenic climate change.

18

19 that ref. S3 uses an equation identical in form to Eq. (S1), but proposes a different, semi-empirical

20 scaling for response time, $\tau \sim \bar{L}/u$, where \bar{L} is the mean-state length and u is a characteristic

21 velocity. Whereas ref. S7 took u to be the speed of kinematic surface waves at the terminus, ref. S3

22 relates u to mass flux and, via a scale analysis, to simple functions of glacier geometry, then finally
23 calibrating it to the output of numerical models. Ref. S1 demonstrates that the original scaling of
24 ref. S2 ($\tau = -H/b_t$) better captures glacier dynamics. But regardless, since there is uncertainty
25 in H we include a broad uncertainty in our estimates of τ . In the next sections we derive two
26 independent ways to estimate the signal-to-noise ratio of glacier length.

27 **2 The PDF of the null hypothesis in the presence of climatic per-** 28 **sistence**

29 As noted in the main text and methods, we evaluated our modeled mass-balance time series, $b'(t)$,
30 for the presence of persistence (i.e., autocorrelations in time, after linear detrending). 34 of the 37
31 mass-balance time series were consistent with white noise. However studies have shown that if per-
32 sistence were present, it would enhance $\sigma_L^{S8,S9}$. Various statistical models exist for representing such
33 persistence. Ref. S9 showed that so-called ‘power-law’ persistence of the form $P(f) = P_0(f/f_0)^{-\eta}$,
34 where $P(f)$ is the spectral power as a function of frequency f , had the largest impact on σ_L .
35 Taking Hintereisferner again as an example, we find the power spectrum of the detrended $b'(t)$
36 is characterized by $\eta = 0.15 \pm 0.2$ (95% bounds), which is not statistically significant and thus
37 consistent with the autoregression tests. Nevertheless we can take a what-if approach: in the event
38 such persistence were present, what would the be impact on our conclusions? Following ref. S9 we
39 generate long synthetic mass-balance times series in which power-law persistence is present (but
40 with no underlying climate trend), and determine the null probability distribution of the ΔLs that
41 arise in arbitrary 130 yr time periods as a result of this random climate variability. Fig. S2 shows
42 the resulting PDFs for the parameters appropriate for Hintereisferner. Adding persistence does

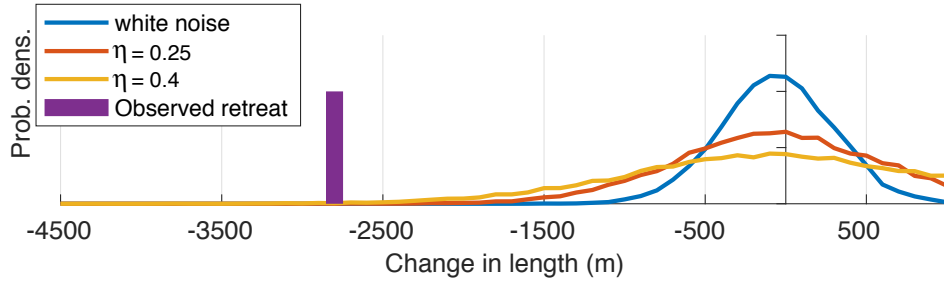


Figure S2: The impact of persistence on the null probability distribution of ΔL for Hintereisferner. The curves show the PDFs of ΔL s that occur for arbitrary 130-yr segments of long synthetic climate time series in which varying amounts of persistence of the form $P(f) = P_0(f/f_0)^{-\eta}$ have been added, but with no trend; and compared to the observed retreat of Hintereisferner. PDF areas are normalized to 1.

43 broaden the distribution of $\Delta L|^{null}$. However, even for the extreme case of $\eta = 0.4$, the probabil-
 44 ity of the observed glacier retreat remains less than 1%. Thus our conclusion that it is ‘*virtually*
 45 *certain*’ the observed retreat required a climate change remains the same.

46 3 Application to a global distribution of glaciers

47 We apply our analysis to 37 glaciers across five geographic regions (the Alps, Scandinavia, North
 48 America, Asia, the Southern Hemisphere). Data for glacier length comes from ref. S6; and for mass
 49 balance from the World Glacier Monitoring Service (WGMS)^{S10}, unless otherwise noted in the SI
 50 spreadsheet. The two other key factors are b_t , the annual mass balance at the terminus, and H the
 51 characteristic thickness near the terminus. We draw on a variety of sources for these, but primarily
 52 b_t is taken from vertical mass-balance profiles reported by WGMS; where possible H is taken from
 53 observed or modeled glacier profiles, otherwise we use the thickness scalings provided by ref. S11
 54 and S12, from which H can be estimated from other geometric glaciers parameters provided by the
 55 WGMS^{S10}.

56 In the supplementary spreadsheet, the complete set of parameters for all 37 glacier are provided,
 57 along with their sources (refs. S10 to S43). We preferentially selected valley glaciers with long
 58 mass-balance records (or long records from nearby glaciers), and continuous length histories without
 59 long gaps. We could not always satisfy these conditions, particularly for glaciers in Asia and South
 60 America, which typically have sparse length histories. For 16 of the 37 glaciers the length records
 61 are too sparse to determine the degrees of freedom (these glaciers are indicated in SI spreadsheet),
 62 and for these we stipulate a flat, negative definite prior on s_L . This choice for $h_{s_L}|^{L_{obs}}$ is consistent
 63 with the observed retreat ($\Delta L < 0$) of all these glaciers (Figs. 1 and S3 to S7); and also with the
 64 modeled negative mass balance (due primarily to the observed warming trends, all of which are
 65 significant at the 5% level). Characteristic glacier response times of several decades mean we can be
 66 certain that, despite only having sparse observations, we have not mistakenly identified as a retreat
 67 what was actually an overall advance. In many instances this can be verified by evidence that is
 68 additional to the formal length measurements including aerial photography, historical records, and
 69 geomorphic analysis. Given $\Delta L < 0$, and since σ_L is positive definite, $s_L|^{obs}$ must be negative.
 70 Further, this flat PDF allows the possibility that s_L is arbitrarily close to zero, which implies
 71 arbitrarily large σ_L . When combined with our climate-based PDF, $h_{s_L}(s_L)|^{T, P_{obs}}$, our analyses for
 72 several glaciers do indeed show upper bounds (97.5%) of $\sigma_L \gg 1$ km (Fig. 1, S3 to S7, and SI
 73 spreadsheet). The potential for such large σ_L acts to increase p_L^{null} (the probability the observed
 74 retreat could have happened in a constant climate). However, it is likely that such large values
 75 for σ_L can be ruled out on physical grounds, particularly for arid climates and smaller glaciers.
 76 Although not part of our analyses here, analytical (i.e., Eq. 6) or numerical modeling that included
 77 parameter uncertainty would help constrain σ_L , and would very likely further decrease p_L^{null} in
 78 these cases.

79 For completeness, for all glaciers we report the statistical significance evaluated using both the full
 80 analyses (i.e., combining $h_{s_L}|^{L_{obs}}$ and $h_{s_L}|^{T,P_{obs}}$ using Bayes' theorem), and also stipulating a flat,
 81 negative-definite prior for $h_{s_L}|^{L_{obs}}$ instead. Finally, for clarity, we also present the results of the
 82 analysis graphically for all five regions (Figs. S3 to S8).

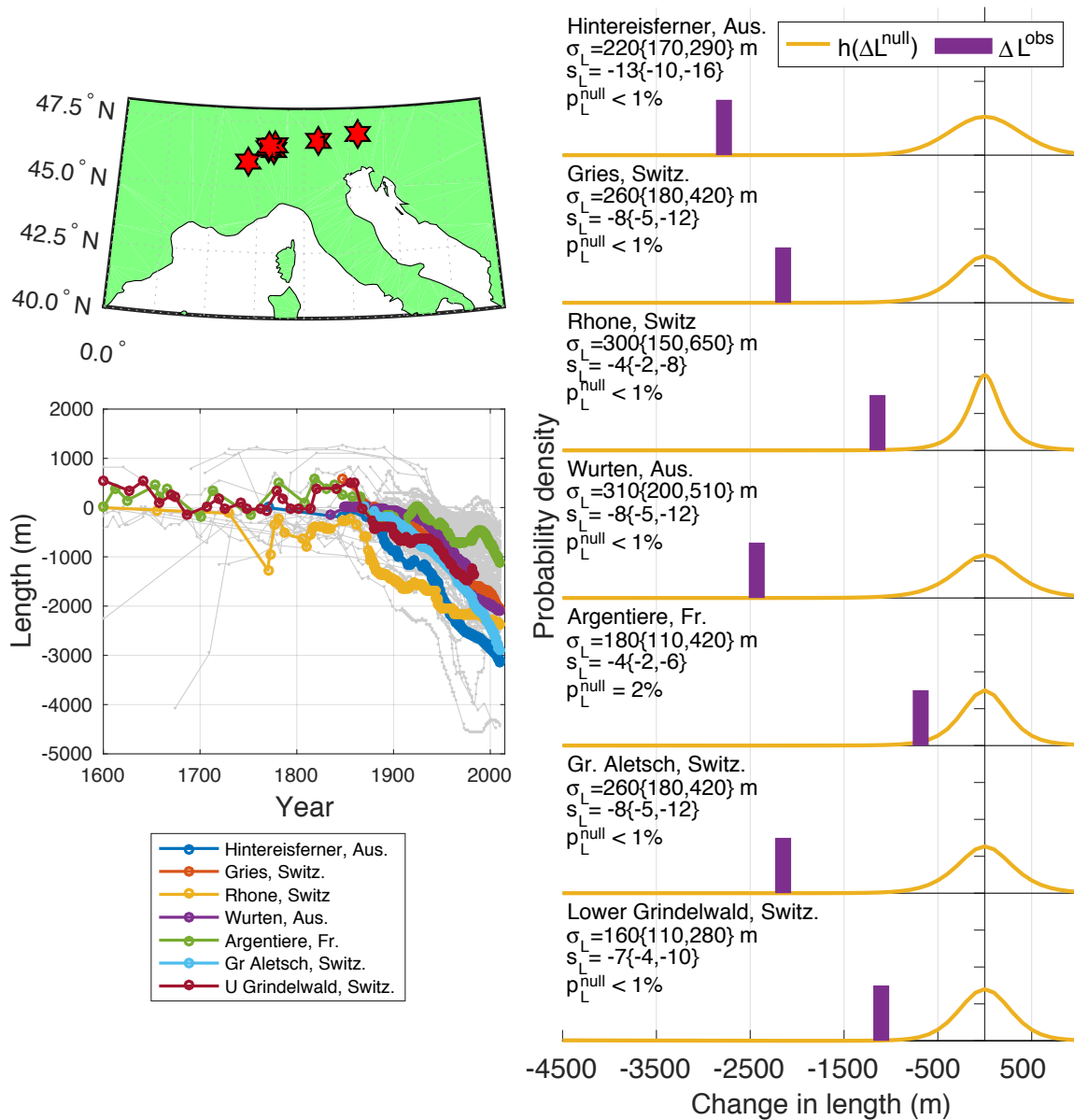


Figure S3: Glacier analyses in the European Alps. The top left panel show the locations of the glacier analyzed. The bottom left panel shows the length histories and length histories of the glaciers analyzed. Right panels are as for Fig. 4.

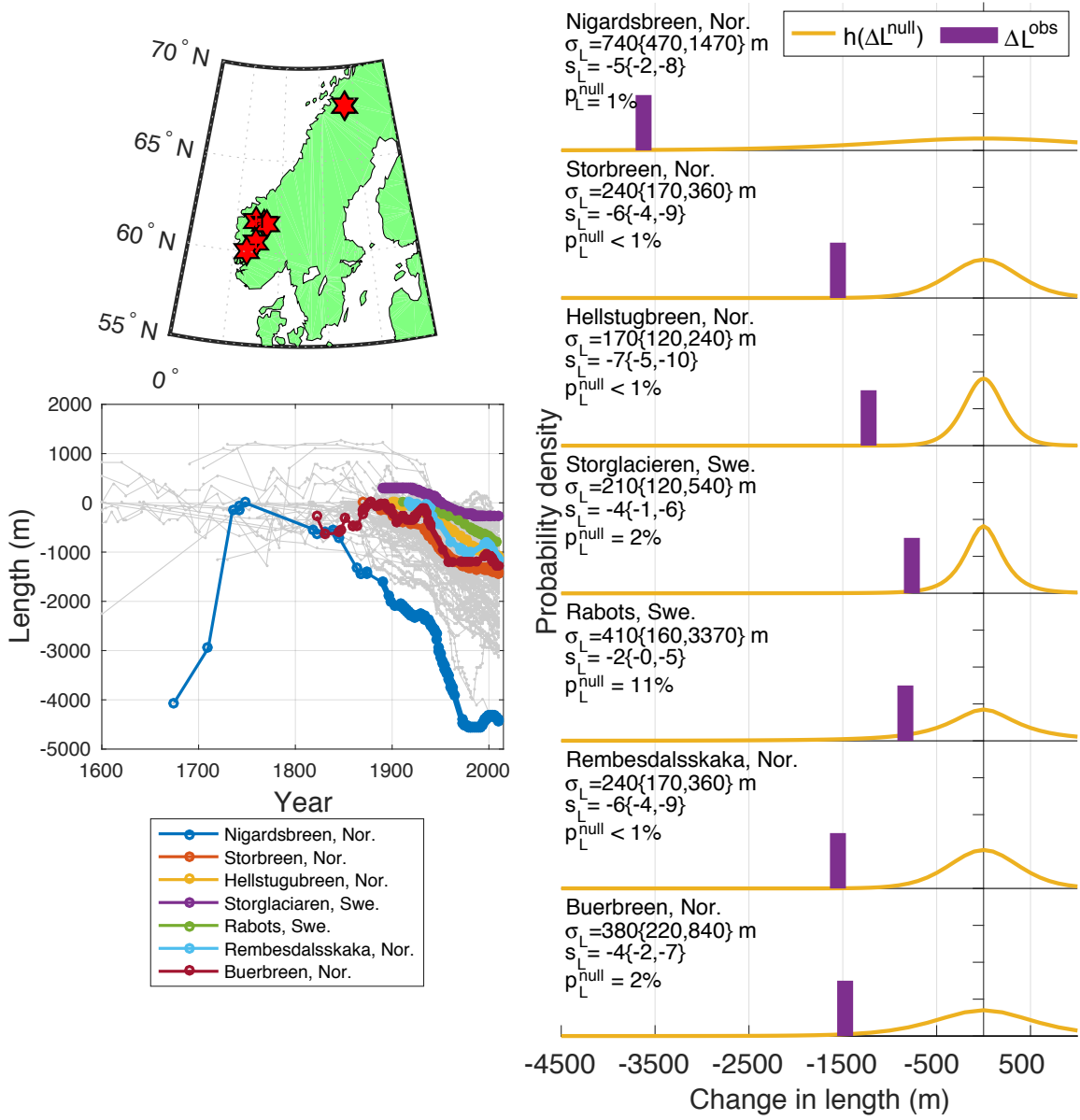


Figure S4: As for Fig. S3, but for analyzed glaciers in Scandinavia.

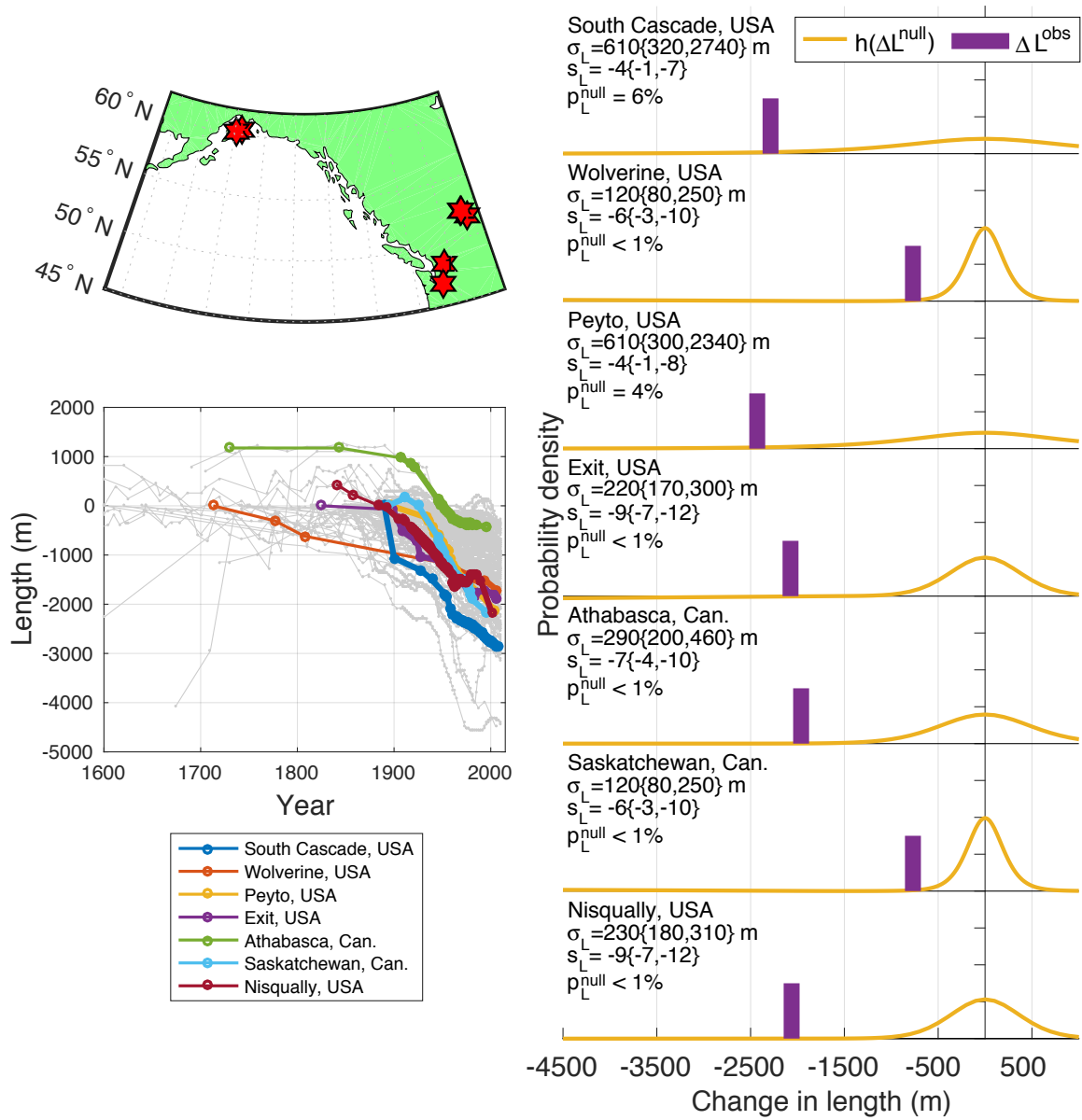


Figure S5: As for Fig. S3, but for analyzed glaciers in North America.

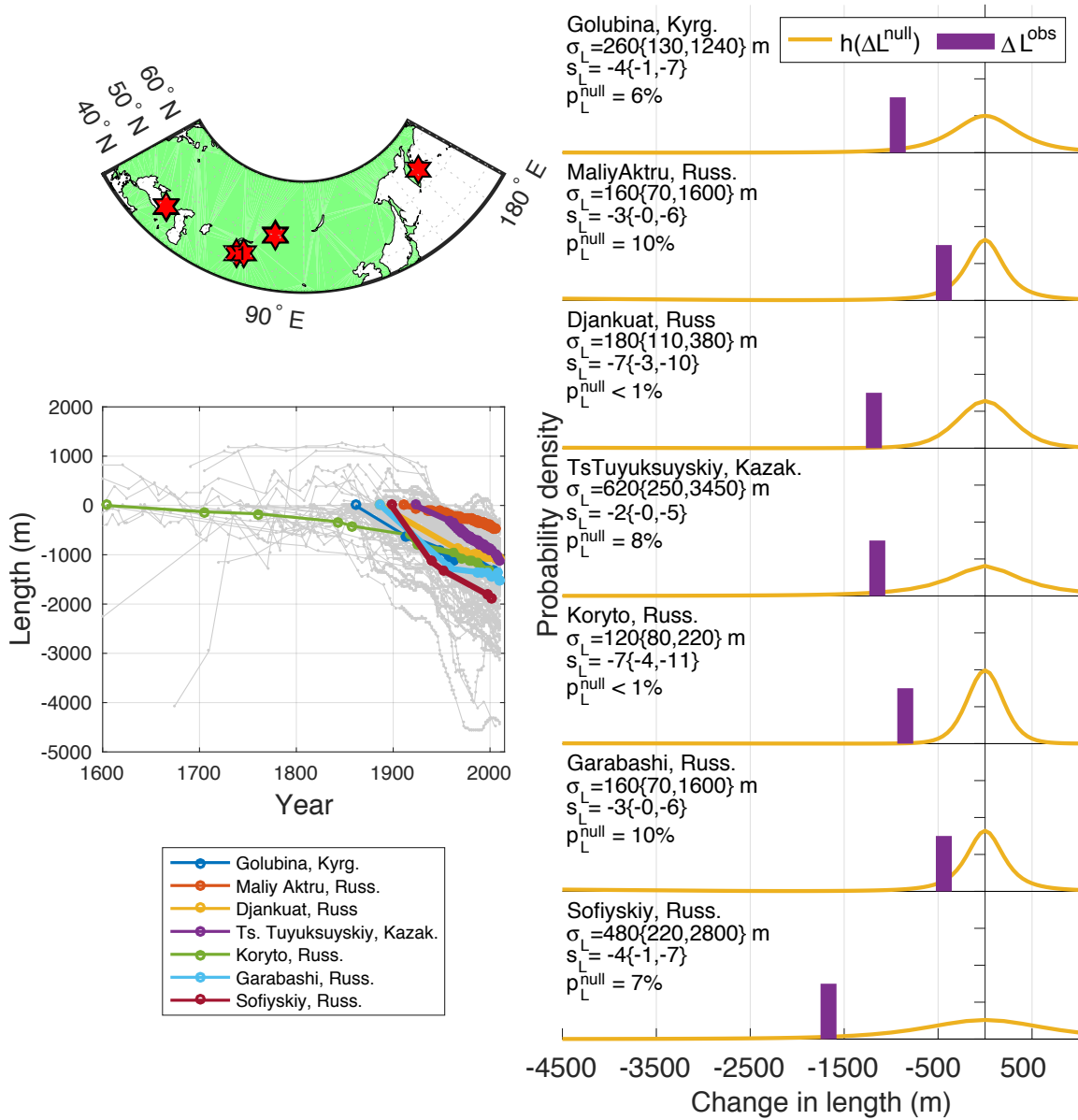


Figure S6: As for Fig. S3, but for analyzed glaciers in Asia.

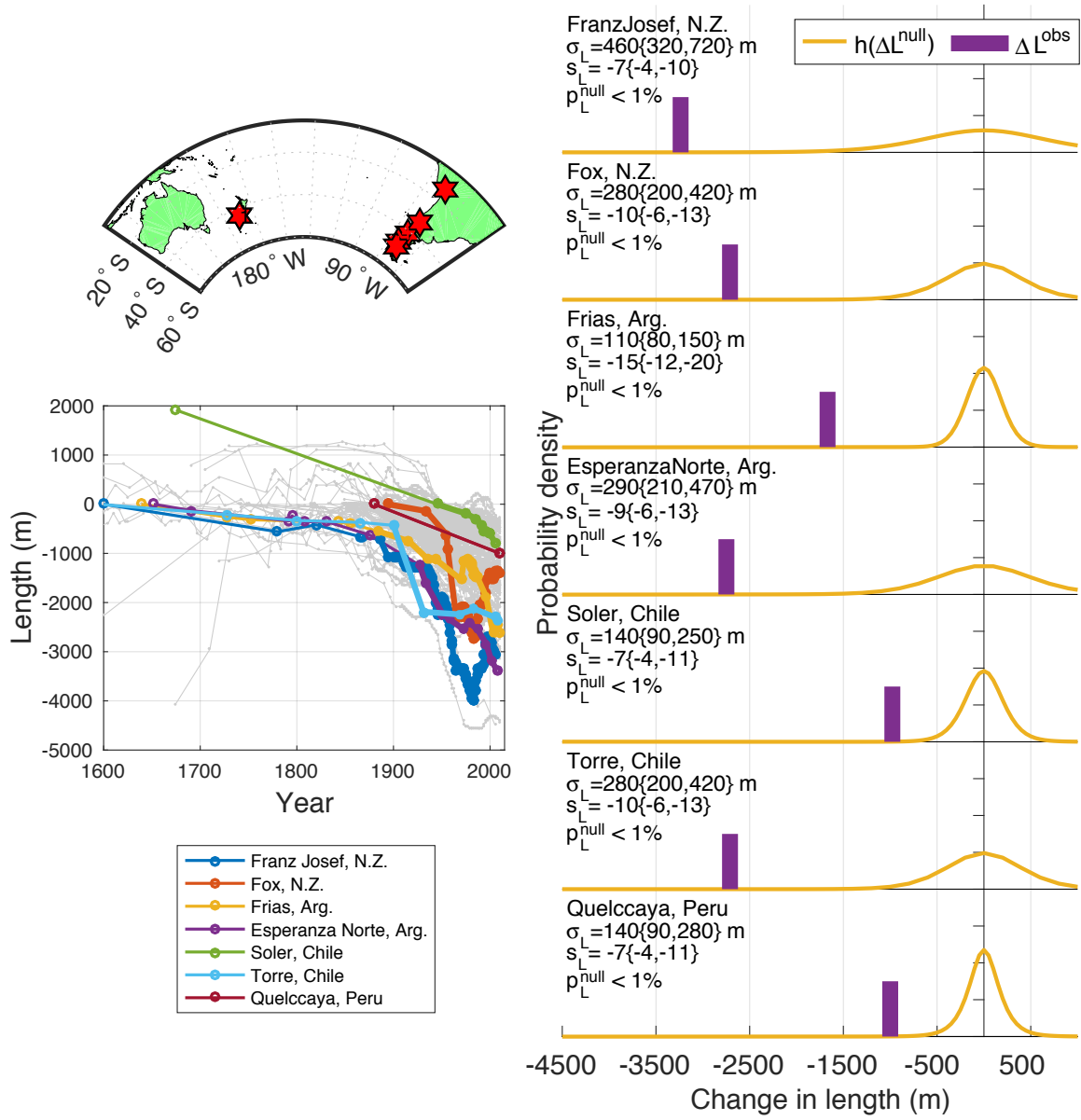


Figure S7: As for Fig. S3, but for analyzed glaciers in the Southern Hemisphere.

83 **References:**

- 84 S1. Roe., G.H. & Baker, M. B. Glacier response to climate perturbations: an accurate linear
85 geometric model. *J. Glaciol.* **60**, 670-684 (2014).
- 86 S2. Jóhannesson, T., Raymond, C. F. & Waddington, E. D. Timescale for adjustments of glaciers
87 to changes in mass balance. *J. Glaciol.* **35**, 355-369 (1989).
- 88 S3. Oerlemans, J., *Glaciers and climate change*. Lisse, etc., A.A. Balkema (2001).
- 89 S4. Oerlemans, J. Extracting a climate signal from 169 glacier records. *Science* **308**, 675-677
90 (2005).
- 91 S5. Raper, S. C. B. & Braithwaite, R. J. Glacier volume response time and its links to climate and
92 topography based on a conceptual model of glacier hypsometry. *The Cryosphere* **3**, 183-194
93 (2009).
- 94 S6. Leclercq, P.W. & Oerlemans, J. Global and hemispheric temperature reconstruction from 491
95 glacier length fluctuations. *Clim. Dyn.* **38**, 1065-1079 (2011).
- 96 S7. Nye, J .F. The response of glaciers and ice sheets to seasonal and climatic changes. *Proc. R.*
97 *Soc. London. Ser. A* **256**, 559-584 (1960).
- 98 S8. Reichert, B.K., Bengtsson, L. & Oerlemans, J. Recent glacier retreat exceeds internal vari-
99 ability. *J. Climate* **15**, 3069-3081 (2002).
- 100 S9. Roe, G.H. & and Baker, M.B. The response of glaciers to climatic persistence. *J. Glaciology*
101 DOI: 10.1017/jog.2016.4 (2016)
- 102 S10. WGMS. *Fluctuations of Glaciers Database*. World Glacier Monitoring Service, Zurich, Switzer-
103 land. DOI:10.5904/wgms-fog-2014-09. Online access: <http://dx.doi.org/10.5904/wgms-fog->

- 104 2014-09 (2014).
- 105 S11. Haeberli, W. & Hoelzle, M. Application of inventory data for estimating characteristics of
106 and regional climate-change effects on mountain glaciers: a pilot study with the European
107 Alps. *Ann. Glaciol.* **21**, 206-212 (1995).
- 108 S12. Hoelzle, M., Chinn, T., Stumm, D., Paul, F., Zemp, M. & Haeberli W. The application of
109 glacier inventory data for estimating past climate change effects on mountain glaciers: A
110 comparison between the European Alps and the Southern Alps of New Zealand. *Glob. and*
111 *Plan. Change* **56(12)**, 69-82 (2007).
- 112 S13. Greuell, W. Hintereisferner, Austria: mass-balance reconstruction and numerical modelling
113 of the historical length variations. *J. Glaciology* **38**, 233-244 (1992).
- 114 S14. Schlosser, E., Numerical simulation of fluctuations of Hintereisferner, Ötztal Alps, since ad
115 1850. *Ann. Glaciol.* **24**, 199-202 (1996).
- 116 S15. Schwitter, M.P. & Raymond, C. F. Changes in the longitudinal profiles of glaciers during
117 advance and retreat. *J. Glaciol.* **39(133)**, 582-590 (1993).
- 118 S16. Woo, M. & Fitzharris B. B. Reconstruction of mass-balance variations for Franz Josef Glacier,
119 New Zealand. *Arct. Alp. Res.* **24**, 281-290 (1992).
- 120 S17. Anderson, B., Lawson, W., & Owens, I. Response of Franz Josef Glacier *Ka Roimata o Hine*
121 *Hukatere* to climate change. *Glob. Plan. Change* **63**, 23-30 (2008).
- 122 S18. Oerlemans, J. Climate sensitivity of Franz Josef Glacier, New Zealand, as revealed by numer-
123 ical modelling. *Arctic and Alpine Research* **29**, 233-239 (1997).
- 124 S19. Leclercq, P. W., Pitte, P., Giesen, R. H., Masiokas, M. H. & Oerlemans, J. Modelling and
125 climatic interpretation of the length fluctuations of Glaciar Frías (north Patagonian Andes,

- 126 Argentina) 1639-2009 AD. *Climate of the Past* **8**, 1385-1402, doi: 10.5194/cp-8-1385-2012
127 (2012).
- 128 S20. Van Beusekom, A. E., O'Neel, S. R., March, R. S., Sass, L. C. & Cox, L. H. Re-analysis of
129 alaskan benchmark glacier mass-balance data using the index method. *US Geological Survey*
130 *Scientific Investigations Report* **5247**, 16 (2010).
- 131 S21. Clarke, G. K. C., Anslow, F. S., Jarosch, A. H., Radic, V., Menounos, B., Bolch, T. & Berthier,
132 E. Ice volume and subglacial topography for western Canadian glaciers from mass balance
133 fields, thinning rates, and a bed stress model. *J. Climate* **26**, 4282-4303. doi:10.1175/JCLI-
134 D-12-00513.1 (2013).
- 135 S22. Meier, M. F. & Post, A. Recent variations in mass net budgets of glaciers western North
136 America. *IUGG/IAHS Pub.* **58**, 63-77 (1962).
- 137 S23. Meier, M.F., Rigsby, G. P. & Sharp, R. P. Preliminary data from Saskatchewan Glacier,
138 Alberta, Canada. *Arctic* **7**, 3-26 (1954).
- 139 S24. Rasmussen, L.A. & Wenger, J. M. Upper-air model of summer balance on Mt. Rainier, USA.
140 *J Glaciology* **55**, 619-624 (2009).
- 141 S25. Yamaguchi, S., Naruse, R. & Shiraiwa, T. Climate reconstruction since the Little Ice Age
142 by modelling Koryto glacier, Kamchatka Peninsula, Russia. *J. Glaciology* **54(184)**, 125-130
143 (2008).
- 144 S26. Pattyn, F., De Smedt, B., De Brabander, S., Van Huele, W., Agatova, A., Mistrukov, A. &
145 Declair, H. Ice dynamics and basal properties of Sofiyskiy Glacier, Altai Mountains, Russia
146 based on DGPS and radio-echo sounding surveys. *Ann. Glaciol.* **37**, 286-292 (2003).

- 147 S27. Cherkasov, P. A., Ahmetova, G. S., & Hastenrath, S. Ice flow and mass continuity of Shumsky
148 Glacier in the Djungarski Alatau Range of Kazakhstan, Central Asia. *J. Geophys. Res.* **101**,
149 12,913-12,920 (1996).
- 150 S28. Grove J. M. *Little Ice Ages: Ancient and Modern. Second edition.* London and New York:
151 Routledge, 2 vols (2004).
- 152 S29. Schaefer, M., Machguth, H., Falvey, M. and Casassa, G. Modeling past and future surface
153 mass balance of the Northern Patagonia Icefield, *J. Geophys. Res. Earth Surf.*, **118**, 571-588,
154 doi:10.1002/jgrf.20038 (2013).
- 155 S30. Popovnin, V. V., Danilova, T. A. & Petrakov, D. A. A pioneer mass balance estimate for a
156 Patagonian glacier: Glaciar de los Tres, Argentina.]*Global and Planetary Change* **22**, 255-267
157 (1999).
- 158 S31. Kelly, M. A., Lowell, T. V., Applegate, P. J., Smith C. A., Phillips, F. M., & Hudson, A.
159 M. Late glacial fluctuations of Quelccaya Ice Cap, southeastern Peru. *Geology* **40**, 991-994
160 (2012).
- 161 S32. Malone A. G. O., Pierrehumbert, R. T., Lowell, T. V., Kelly, M. A. & Stroup, J. S. Constraints
162 on southern hemisphere tropical climate change during the Little Ice Age and Younger Dryas
163 based on glacier modeling of the Quelccaya Ice Cap, Peru. *Quat. Sci. Rev.* **125**, 106-116
164 (2012).
- 165 S33. Purdie, H., Brook, M. & Fuller, I. Seasonal variation in ablation and surface velocity on a
166 temperate maritime glacier: Fox Glacier, New Zealand. *Arct. Antarct. Alp. Res.* **40(1)**,
167 140-147 (2008).
- 168 S34. Chen, J. & Funk, M. Mass Balance of Rhonegletscher during 1882/83-1986/87. *J. Glaciology*

- 169 **36(123)** 199-209 (1990).
- 170 S35. Goehring, B. M., Vacco, D. A., Alley, R. B. & Schaefer, J. M. Holocene dynamics of the
171 Rhone Glacier, Switzerland, deduced from ice flow models and cosmogenic nuclides. *Earth
172 and Planetary Science Letters* **351-352**, 27-35 (2012).
- 173 S36. Juvet, G., Huss, M., Funk, M. & Blatter, H. Modelling the retreat of Grosser Aletschgletscher,
174 Switzerland, in a changing climate. *J. Glac.* **57(206)**, 1033-1046 (2011).
- 175 S37. Huss, M., Bauder, A., Funk M. & Hock, R. Determination of the seasonal mass balance of four
176 Alpine glaciers since 1865. *J. Geophys. Res.* **113(F1)**, doi:10.1029/2007JF000803 (2008)
- 177 S38. Huybrechts, P., de Nooze, P. & Declerq, H. Numerical modelling of Glacier d'Argentire and its
178 historic front variations. In Oerlemans, J., editor, *Glacier fluctuations and climatic change*,
179 Dordrecht: Kluwer Academic Publishers, 373-389 (1989).
- 180 S39. Schmeits, M. J. & Oerlemans, J. Simulation of the historical variation in length of the Unterer
181 Grindelwaldgletscher, Switzerland. *J. Glac.* **43(143)**, 152-164 (1997).
- 182 S40. Andreassen, L. M., Huss, M., Melvold, K., Elvehøy, H. & Winsvold, S. H. Ice thickness
183 measurements and volume estimates for glaciers in Norway. *J. Glac.* **61(228)**, 763-775
184 (2015).
- 185 S41. Stroeven, A. P. The robustness of one-dimensional, time-dependent, ice-flow models: A case
186 study from Storglaciären, northern Sweden. *Geogr. Ann.* **78 A (2-3)** 133-146 (1996).
- 187 S42. Björnsson, H. Radio-echo sounding maps of Storglaciären, Isfallsglaciären and Rabots glaciär,
188 northern Sweden. *Geogr. Ann.* **63 A (3-4)** 225-231 (1981).
- 189 S43. Giesen, R. H. & J. Oerlemans, J. Response of the ice cap Hardangerjøkulen in southern
190 Norway to the 20th and 21st century climates. *Cryosphere* **4(2)**, 191-213 (2010).